

## REFRACTIVE INDEX DEPENDENCE ON OPTICAL GAP IN AMORPHOUS SILICON—PART I. Si PREPARED BY GLOW DISCHARGE

N. M. RAVINDRA, C. ANCE, S. P. COULIBALY, F. DE CHELLE, J. M. BERGER,  
J. P. FERRATON and A. DONNADIEU

Laboratoire de Spectroscopie II, Equipe de Recherche Associée au C.N.R.S., Université des Sciences et  
Techniques du Languedoc, Place Eugène Bataillon, 34060 Montpellier Cedex, France

(Received 4 January 1983; accepted 25 January 1983)

**Abstract**—We present here our studies concerning the variation of refractive index with the optical gap in amorphous silicon prepared by glow discharge decomposition of silane. The study has been carried out in the light of the models of Penn, Wemple-Didomenico, Ravindra *et al.*, Moss and Bahl-Bhagat. It is essentially seen that the model of Bahl-Bhagat is good enough to explain the relative shifts in the refractive indices in terms of the changes in the gaps on introduction of hydrogen into amorphous silicon. However, because of weaknesses associated with the fitting parameters, we propose here an alternate model which explains fairly well the dependence of the index of refraction on the optical gap. Furthermore, to explain the gradient of the refractive index vs optical gap plots, we see that a simple model like that of Moss would suffice. This is all the more interesting by virtue of the fact that the Moss formula is basically representative of the atomic picture. Of course, the constant depends on conditions during formation of the sample. Under some limiting conditions, the Bahl-Bhagat relation is shown to reduce to the linear form like that of Ravindra *et al.* We also attempt to analyse qualitatively the dependence of dispersion energy and the average excitation energy on temperature in the light of the Wemple-Didomenico model. The present study has been carried out for samples prepared by glow discharge at different substrate temperatures and with different hydrogen concentrations.

### INTRODUCTION

Today, amorphous silicon enjoys a privileged position as a material of outstanding interest both from the material and device point of view. Interest in this material has been further enhanced by virtue of the fact that all the hopes and aspirations of device physicists working in the area of solar energy conversion seems to be pinned on amorphous silicon—as a possible viable alternative to crystalline silicon. But, fortunately or unfortunately, the properties of amorphous silicon are influenced to a great extent by the method of preparation and conditions during preparation of the film. This is particularly the case with the refractive index and the optical gap. Various attempts have been made to explain the variation of refractive index with the optical gap. The most accepted model for amorphous silicon has been the model of Bahl and Bhagat.<sup>(1)</sup>

Bahl and Bhagat<sup>(1)</sup> attributed the changes in refractive index to variations in the optical gap. However, their model was proposed for evaporated amorphous Si. In this presentation, we essentially attempt to extrapolate the Bahl-Bhagat relation to amorphous silicon produced by glow discharge. While attempting to do so, we run into difficulties. We wish to point out here that such an extrapolation was done earlier by Martin and Pawlewicz<sup>(2)</sup> to a-Si:H alloys produced by sputtering. These difficulties arise mainly because of the definition of Bahl-Bhagat for the fitting parameters appearing in their relation. Hence, we propose an alternate model which in our opinion seems to be more consistent. We also examine the validity of Penn-like models<sup>(3)</sup> and the model of Wemple-Didomenico<sup>(4)</sup> in the light of the work of Ravindra *et al.*<sup>(5)</sup> The parameters involved in the Wemple-Didomenico model and their temperature dependences are then analysed. In general, the experimental results are shown to obey the well known Moss formula.<sup>(6)</sup> However, the constant is seen to be dependent on the hydrogen concentration.

### EXPERIMENTAL DETAILS IN BRIEF

For details concerning the preparation of the film and the measurement of the optical properties, see Refs (7-9). Essentially, the absorption coefficient  $\beta$  for the film was evaluated from experimental

measurements of reflectance and transmittance. The optical gap was determined from a plot of  $(\beta h\nu)^{1/2}$  vs  $h\nu$  where the symbols have their usual meanings. The refractive index was calculated from the wavelength corresponding to the extremum of the interferences occurring in the reflectivity and transmittivity. The measurement temperature  $T_m$  was controlled with a thermostat and was noted using a Pt–Pt Rh thermocouple.

### THEORY AND DISCUSSION

Based on the fundamental equation relating the low frequency refractive index to the frequency dependent absorption,<sup>(10)</sup>

$$n - 1 = (c/2\pi^2) \int_0^\infty |\beta(v)/v^2| dv \quad (1)$$

in their detailed studies of the dependence of the properties of amorphous silicon films on deposition conditions, Bahl and Bhagat<sup>(1)</sup> have earlier presumed that in an energy range  $|E_g, E_h|$ ,

$$(\beta E)^{1/2} = \gamma (E - E_g) \quad (1a)$$

where  $\beta$  is the absorption coefficient and  $\gamma$  is the slope of the  $(\beta E)^{1/2}$  vs  $E$  plot.

Integration of equation (1) in the limits  $E_g < E < E_h$  and  $E > E_g$  leads to an expression of the form<sup>(8)</sup>

$$n = A \left| \ln E_g - 2 \frac{E_g}{E_h} + \frac{1}{2} \left( \frac{E_g}{E_h} \right)^2 \right| + B \quad (2)$$

where  $A = -(hc\gamma^2)/(2\pi^2)$  and  $B$  is a constant.  $E_h$  has the same meaning as in the Bahl–Bhagat model.

Here, we suppose that the contribution to the index of refraction  $n$  due to states of energy  $E > E_h$  is roughly a constant. If we refer to the first term on the right as  $\Delta n$ , that is the contribution to  $n$  due to states of energy  $E_g < E < E_h$ , then the Bahl–Bhagat relation may be written as

$$\Delta(\Delta n) = -(c\gamma^2 h/2\pi^2 E_g) (1 - E_g/E_h)^2 \Delta E_g \quad (3)$$

where the symbols have their usual meanings (see Ref. 1 for details).

Of particular importance here are the parameters  $E_h$  and  $\gamma$  which have been defined respectively as follows. Bahl and Bhagat<sup>(1)</sup> suggest that

$$E_h - E_g \cong 10 \text{ eV} \cong \Delta E_{VB} \quad (4)$$

where,  $\Delta E_{VB}$  represents the width of the valence band in silicon.  $\gamma$  [ $\cong 500(\text{cm eV})^{-1/2}$ ] is the slope of the  $\sqrt{(\beta h\nu)}$  vs  $h\nu$  plot. Further, incorporating the values of the constants, it has been shown that to a good approximation, relation (3) may be written as

$$\Delta(\Delta n) = -1.28 (\Delta E_g/E_g) \quad (5)$$

More precisely, the Bahl–Bhagat relation may be written as<sup>(2)</sup>

$$n(0) - n(H) = \delta |E_g(H) - E_g(0)|/E_g(0) \quad (6)$$

for the case of hydrogenated amorphous silicon. Here  $\delta$  is a constant close to unity,  $n(0)$ ,  $n(H)$ , and  $E_g(0)$  and  $E_g(H)$  are the refractive indices and optical band gaps for films containing no hydrogen and hydrogen respectively. In Table 1, we present the results of our calculations based on the Bahl–Bhagat model. As can be seen in the Table,  $E_h$  and  $\gamma$  are dependent on the hydrogen concentration  $C|H|$ . What is all the more intriguing is the fact that, in general,

$$E_h - E_g \ll 10 \text{ eV} \quad (7)$$

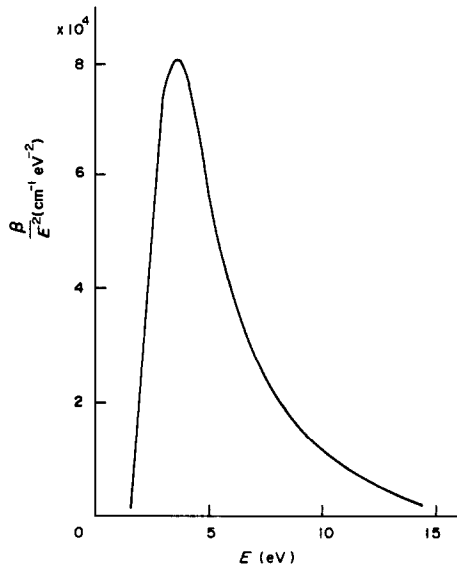
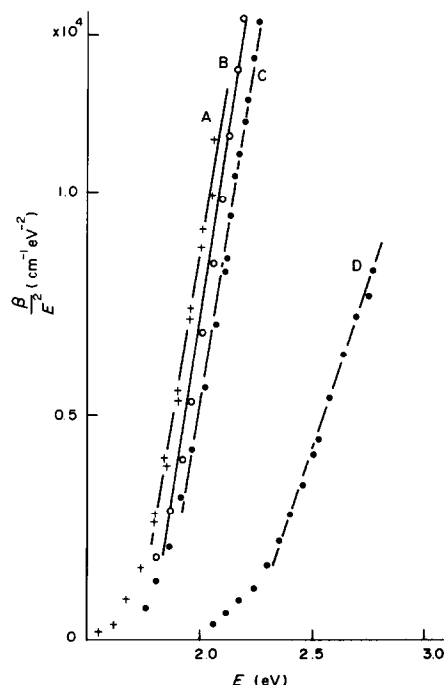
It is this fact that leads us to an examination of the Bahl–Bhagat model.

As a first step in this direction of understanding the Bahl–Bhagat model, we plot in Figs 1a and 1b  $\beta/E^2$  as a function of  $E$ . Figure 1a is essentially based on the data of Pierce and Spicer.<sup>(11)</sup> In Fig. 1a, it can be clearly seen that  $\beta/E^2$  increases linearly, attains a peak at about 4 eV and then

Table 1. Mean values of some of the parameters

$C   H   (\%)$	8	12	17	35
$\hbar\omega_b$ (eV)	16.35	15.24	14.43	13.48
$-\frac{dn}{dE_g}$ (eV $^{-1}$ )	0.82	0.64	0.61	0.27
$n_g/4E_g$ (eV $^{-1}$ )	0.60	0.57	0.50	0.31
$E_g E_0$ (eV $^2$ )	134.4	117.4	106.0	88.9
$-\frac{dn}{dE_g}$ (eV $^{-1}$ )	0.90	0.60	0.69	0.28
$\gamma$ (eV $\cdot$ cm) $^{-1/2}$	680	623	755	517
$E_h$ (eV)	6.30	5.12	4.66	5.23
$A'$ (eV $^{-2}$ )	0.189	0.189	0.189	0.09
$E_K$ (eV)	5.85	4.89	4.81	4.94

f—from the figure.

Fig. 1a.  $\beta/E^2$  as a function of  $E$ .<sup>(11)</sup>Fig. 1b.  $\beta/E^2$  as a function of  $E$  for different hydrogen concentrations (A:  $C | H | = 8\%$ ; B:  $C | H | = 12\%$ ; C:  $C | H | = 17\%$ ; D:  $C | H | = 35\%$ ).

drops down. In Fig. 1b, the linear behaviour is reproduced remarkably well by the samples prepared at different  $C|H|$ . The shift in  $\beta/E^2$  vs  $E$  leads us to believe that there will be a corresponding shift in the peak. Thus the change in hydrogen concentration seems to have altered the position of the peak. Just to make our point of view a little more clear, it would be worthwhile to look at the physical meaning of such a result.

In general, for a-Si:H (hydrogenated amorphous Si), as the hydrogen concentration is increased from 8.0 to 30%, the refractive index  $n$  decreases from 3.5 to 2.4. This has earlier been demonstrated by us for a-Si:H films produced by glow discharge.<sup>(12)</sup> Thus, according to the Clausius–Mossotti relation (or the Lorentz–Lorenz relation), as  $n$  decreases, the electronic polarizability should also decrease.<sup>(2)</sup> This is very consistent with the accepted model for hydrogen binding in amorphous silicon. At high hydrogen concentrations, the SiH<sub>n</sub> structures have low polarizabilities compared to SiH structures formed at low hydrogen concentrations. Thus, this explains the low refractive index at high hydrogen concentrations. Such a conclusion also follows from the Bahl–Bhagat model.

Bahl–Bhagat attribute the variations in  $n$  to changes in the position of the fundamental absorption edge. The increase in  $n$  was further explained in terms of the spin density for the films. These results could be extrapolated to hydrogenated amorphous Si without any difficulty. After all, an increase in hydrogen concentration saturates more of the bonds (which would otherwise be dangling) thereby decreasing the spin density and thus lowering  $n$ . Thus, the Bahl–Bhagat model (BBM) explains the results reasonably well. However, quantitatively speaking, we are faced with difficulties. It seems logical to assume that the parameter  $E_h$  is of utmost importance in the Bahl–Bhagat relation (BBR). What does not seem to be logical is the definition of  $E_h$  (equation 4). So, essentially according to the BBM,  $E_h$  must exceed 10 eV. For optical transitions in the visible region or even in the u.v., the contributions from states near the gap are the most dominant ones. As such, the width of the valence band does not seem to play a significant role in optical transitions.

These conclusions coupled with those based on Figs 1a and 1b lead us to propose an alternate model which in our opinion seems to be physically more consistent. Based on our experimental results (Fig. 1b), we define

$$\frac{\beta}{E^2} \propto (E - E_g) \quad (8)$$

Using the above condition (8) in equation (1), after carrying out integration in the limit  $E_g$  to  $E_K$  and then differentiating, we obtain

$$\frac{\Delta n}{\Delta E_g} = A'(E_g - E_K) \quad (9)$$

where

$$A' = \left( \frac{hc}{2\pi^2} \right) a = 62.88 \times 10^{-7} a \quad (10)$$

and  $a$  is the slope of  $\beta/E^2$  vs  $E$  plot (in the linear part),  $E_K$  representing the energy corresponding to the peak of the plot. In Table 1, we report the results of our calculations based on equation (9). As can be seen in the table,  $E_K$  takes a value around  $5 \pm 1$  eV. Thus, in our opinion, to explain the shift in the index of refraction with the shift in the gap, equation (9) seems to be more reasonable than the BBR (equation 6). Essentially, our proposed relation (equation 9) is similar to the BBR. After all, the parameters  $\gamma$  and  $E_h$  may be treated as analogous to  $A'$  and  $E_K$ , respectively. But,  $E_K$  has been associated with the peak of  $\beta/E^2$  vs  $E$  plot and has nothing to do with the width of the valence band.

At this stage, it would be worthwhile to look at the applicability of other models to explain the dependence of  $n$  on  $E_g$ . We wish to confess here that with the type of study being presented here, it is rather difficult to look at the microscopic or fine structure aspects concerning the effect of hydrogenation.

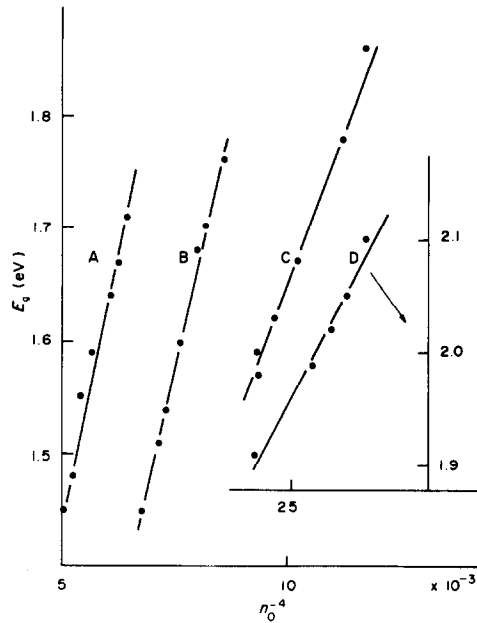


Fig. 2. Plot of  $E_g$  against  $1/n_0^4$  as a function of the measurement temperature  $T_m$  for different  $H_2$  concentrations.

Based on the fundamental principle that in a dielectric medium, all energy levels are scaled down by a factor  $\epsilon^2$  or  $n^4$ , Moss<sup>(6,10)</sup> proposed the famous relation

$$E_g n^4 = \text{constant} \quad (11)$$

In Fig. 2, we plot  $E_g$  as a function of  $(1/n)^4$ . As can be seen in the figure, our experimental results obey the Moss formula fairly well. This is all the more encouraging especially because of the fact that the Moss formula is essentially based on an atomic model. Further, from Fig. 2, it follows that  $E_g$  varies as

$$E_g = m(1/n)^4 + C \quad (12)$$

where  $m$  is the slope and  $C$  is the intercept. At this stage, we wish to point out that it is the linearity of the  $E_g$  vs  $(1/n)^4$  plot that is of importance rather than necessity of the line passing through the origin, i.e.  $C$  to be zero. Afterall, the present exercise involves an extrapolation of an atomic model to an amorphous system. It may further be seen that  $m$  and  $C$  depend on  $T_s$ .

Secondly, we look at the application of band structural models like Penn<sup>(3)</sup> and Wemple-Didomenico<sup>(4)</sup> to explain the  $n - E_g$  behaviour. For a model semiconductor, the static dielectric constant is given by

$$\epsilon(0) = 1 + \left( \frac{\hbar\omega_p}{E_p} \right)^2 S_0 \quad (13)$$

where  $E_p$  is the Penn gap,  $\omega_p$  is the valence electron plasmon frequency and  $S_0$  is a constant ( $S_0 = 1$  in the original model<sup>(3)</sup>). In the work of Penn,<sup>(3)</sup>  $S_0 = 1$ . Further,  $\omega_p$  is given by

$$\omega_p = \left( \frac{4\pi Ne^2}{m\Omega} \right)^{1/2} \quad (14)$$

where the symbols have their usual meanings. In the above expression (14),  $\Omega$ , the atomic volume, is the only parameter which depends dominantly on temperature. But, even this dependence is small. Thus, in a small temperature range,  $\hbar\omega_p$  may be treated as a constant. Thus, the temperature dependent  $\epsilon(0)$  has a direct reflection on  $E_p$ . Further, an addition of hydrogen implies a decrease in the index of refraction and hence an increase in the Penn gap. We wish to point out here that

our recent studies concerning the annealing effects and hydrogen evolution in amorphous silicon<sup>(13)</sup> indicate that the shift in the Penn gap  $E_p$  with measurement temperature  $T_m$  is the same as that of the optical band gap  $E_g$  with  $T_m$ . That is,

$$\frac{dE_p}{dT_m} \cong \frac{dE_g}{dT_m} \quad (15)$$

It is because of validity of the above definition for amorphous silicon that the work of Martin and Pawlewicz<sup>(2)</sup> is easily understood. In their studies of properties—composition relationships in sputter deposited a-Si:H alloys, Martin and Pawlewicz compare their calculation based on expressions (6) and (13) with their experimental results. Such a comparison holds good by virtue of equation (15). This leads us to a study of the linear relationship proposed by Ravindra *et al.* (see Ref. 5 for details).

Primarily, the scheme developed by Ravindra *et al.*<sup>(5)</sup> is based on a definition,

$$E_p = E_g + K \quad (16)$$

where,  $K$  is a constant. In Tables 2–5 we put the above definition to test. As can be seen in the tables, the above definition (16) is obeyed fairly well for samples prepared with different  $C\{H\}$ . These studies have been carried out at various measurement temperatures  $T_m$ . Using equation (16) in (13), it was further shown<sup>(13)</sup> that  $n$  should vary as

$$n = K_1 - K_2 E_g + K_3 E_g^2 - K_4 E_g^3 \dots \quad (17)$$

where,

$$\begin{aligned} K_1 &= \frac{\sqrt{[E_p^2 + (\hbar\omega_p)^2]}}{(E_p - E_g)} \\ K_2 &= \frac{K_1}{(E_p - E_g)} \\ K_3 &= \frac{K_2}{(E_p - E_g)} \end{aligned} \quad (18)$$

The values of  $K_1, K_2, K_3 \dots$ , are evaluated in Tables 2–5. For a given sample, the constancy of these parameters at various temperatures  $T_m$  is easily seen. This scheme essentially involves binomial expansion and since, for amorphous silicon,  $E_g/K < 1$ , such a scheme is very much valid to explain the refractive index dependence on the optical gap. Of course, one has to consider higher terms in order to explain the correct variation of  $n$  with  $E_g$ . Just as a matter of academic interest, we also attempt in Tables 2–5 the application of the Wemple–Didomenico model.<sup>(4)</sup> As can be seen in the tables, the definition

$$E_0 = E_g + K' \quad (19)$$

is valid for our samples. Here  $E_0$  represents the average excitation energy and  $K'$  is a constant characteristic of the sample. Thus, a similar procedure may be adopted which would again lead us to a relation like equation (17). Based on this kind of analysis, it was further shown that<sup>(14)</sup>

$$n = 4.084 - 0.62 E_g \quad (20)$$

where the constants were essentially attributed to those appearing in relation (17). It is to be noted here that the scheme developed by Ravindra *et al.*<sup>(5,14)</sup> involves an analysis of the  $E_g - n$  data for a large number of semiconductors. Here, we are mainly interested in the extrapolation of this scheme to amorphous Si. Hence we focus our attention only on the slope. In Fig. 3, the  $n$  vs  $E_g$  plots for our samples under study are presented. As can be seen, they are generally linear. From equation (20), it may easily be seen that

$$\frac{dn}{dE_g} = -0.62 \quad (21)$$

Table 2.  $C|\mathbf{H}| = 8\%$  ( $T_s = 623\text{ K}$ )

$T_m$ (K)	$E_g$ (eV)	$n_x$	$E_p$ (eV)	$E_p - E_s$ (eV)	$K_1$	$K_2$	$K_3$	$K_4$	$K_5$	$K_6$	$n_0$	$E_d$ (eV)	$E_0 - E_s$ (eV)	$E_g n_x^4$ (eV)	$E_d E_0$ (eV $^2$ )
95	1.71	3.536	4.82	3.11	5.48	1.76	0.57	0.18	0.06	0.02	3.44	39.2	3.41	1.70	267.3
295	1.67	3.561	4.78	3.11	5.47	1.76	0.56	0.18	0.06	0.02	3.48	39.5	3.38	1.71	268.5
373	1.64	3.584	4.75	3.11	5.47	1.76	0.57	0.18	0.06	0.02	3.51	39.5	3.33	1.69	270.6
473	1.59	3.644	4.67	3.08	5.53	1.80	0.58	0.19	0.06	0.02	3.57	40.5	3.30	1.71	280.4
573	1.55	3.688	4.61	3.06	5.56	1.82	0.60	0.20	0.06	0.02	3.63	41.0	3.25	1.70	286.7
673	1.43	3.777	4.49	3.06	5.54	1.81	0.59	0.19	0.06	0.02	3.74	42.6	3.21	1.78	291.0
Rev*	1.48	3.716	4.57	3.09	5.50	1.78	0.58	0.19	0.06	0.02	3.67	41.6	3.25	1.77	282.2
723	1.33	3.884	4.36	3.03	5.59	1.85	0.61	0.20	0.07	0.02	3.86	43.6	3.10	1.77	302.7
Rev*	1.45	3.749	4.53	3.08	5.52	1.79	0.58	0.19	0.06	0.02	3.71	42.3	3.24	1.79	286.4

 $n_x$ —experimental value of  $n$ . $n_0$ —calculated value of  $n$ .

\*See Ref. (8) for details.

Table 3.  $C|\mathbf{H}| = 12\%$  ( $T_s = 553\text{ K}$ )

$T_m$ (K)	$E_g$ (eV)	$n_x$	$E_p$ (eV)	$E_p - E_s$ (eV)	$K_1$	$K_2$	$K_3$	$K_4$	$K_5$	$K_6$	$n_0$	$E_d$ (eV)	$E_0 - E_s$ (eV)	$E_g n_x^4$ (eV)	$E_d E_0$ (eV $^2$ )
95	1.76	3.287	4.87	3.11	5.15	1.66	0.53	0.17	0.06	0.02	3.18	33.7	3.44	1.68	205.4
295	1.70	3.327	4.80	3.10	5.15	1.66	0.53	0.17	0.06	0.02	3.24	34.2	3.40	1.70	208.3
373	1.68	3.349	4.77	3.09	5.17	1.67	0.54	0.18	0.06	0.02	3.26	34.6	3.39	1.71	211.3
473	1.60	3.385	4.71	3.11	5.13	1.65	0.53	0.17	0.05	0.02	3.32	34.9	3.34	1.74	210.1
573	1.54	3.422	4.66	3.12	5.11	1.64	0.53	0.17	0.05	0.02	3.37	35.4	3.31	1.77	211.2
623	1.51	3.443	4.63	3.12	5.11	1.64	0.53	0.17	0.05	0.02	3.40	36.0	3.32	1.81	212.2
673	1.42	3.491	4.56	3.14	5.07	1.62	0.52	0.16	0.05	0.02	3.46	36.4	3.25	1.83	210.9
Rev*	1.45	3.454	4.61	3.16	5.04	1.60	0.50	0.16	0.05	0.02	3.42	36.0	3.29	1.84	206.4
723	1.26	3.632	4.37	3.11	5.11	1.65	0.53	0.17	0.05	0.02	3.62	37.9	3.11	1.85	219.3
Rev*	1.42	3.507	4.53	3.11	5.11	1.64	0.53	0.17	0.05	0.02	3.48	36.3	3.21	1.79	214.8

 $n_x$ —experimental value of  $n$ . $n_0$ —calculated value of  $n$ .

\*See Ref. (8) for details.

Table 4.  $C|H| = 17\%$  ( $T_s = 553$  K)

$T_m$ (K)	$E_g$ (eV)	$n_x$	$E_p$ (eV)	$E_p - E_g$ (eV)	$K_1$	$K_2$	$K_3$	$K_4$	$K_5$	$K_6$	$n_0$	$E_d$ (eV)	$E_0$ (eV)	$E_0 - E_g$ (eV)	$E_g n_x^4$ (eV)	$E_d E_0$ (eV <sup>2</sup> )
95	1.86	3.042	4.69	2.83	5.04	1.78	0.63	0.22	0.08	0.03	2.80	29.64	3.59	1.73	159.3	106.4
295	1.78	3.074	4.64	2.86	4.99	1.75	0.61	0.21	0.07	0.03	2.89	29.66	3.51	1.73	158.9	104.1
473	1.67	3.148	4.52	2.85	5.00	1.76	0.62	0.22	0.08	0.03	3.02	30.63	3.44	1.77	164.0	105.4
573	1.62	3.187	4.46	2.84	5.00	1.77	0.62	0.22	0.08	0.03	3.08	31.21	3.41	1.79	167.1	106.4
623	1.59	3.219	4.41	2.82	5.04	1.79	0.64	0.23	0.08	0.03	3.12	31.56	3.37	1.78	170.7	106.4
673	1.48	3.277	4.32	2.84	5.00	1.76	0.62	0.22	0.08	0.03	3.21	32.18	3.30	1.82	170.7	106.2
Rev*	1.57	3.218	4.41	2.84	5.00	1.76	0.62	0.22	0.08	0.03	3.13	31.55	3.37	1.80	168.4	106.3
723	1.40	3.340	4.23	2.83	4.99	1.76	0.62	0.22	0.08	0.03	3.29	32.87	3.24	1.84	174.2	106.3
Rev*	1.59	3.249	4.36	2.77	5.11	1.85	0.67	0.24	0.09	0.03	3.13	31.82	3.34	1.75	177.2	106.3

 $n_x$ —experimental value of  $n$ . $n_0$ —calculated value of  $n$ .

\*See Ref. (8) for details.

Table 5.  $C|H| = 35\%$  ( $T_s = 323$  K)

$T_m$ (K)	$E_g$ (eV)	$n_x$	$E_p$ (eV)	$E_p - E_g$ (eV)	$K_1$	$K_2$	$K_3$	$K_4$	$K_5$	$K_6$	$n_0$	$E_d$ (eV)	$E_0$ (eV)	$E_0 - E_g$ (eV)	$E_g n_x^4$ (eV)	$E_d E_0$ (eV <sup>2</sup> )
95	2.10	2.475	5.95	3.85	3.82	0.99	0.26	0.07	0.02	0.004	2.41	21.73	4.24	2.14	78.8	92.1
295	2.05	2.485	5.93	3.88	3.80	0.98	0.25	0.07	0.02	0.004	2.43	21.70	4.19	2.14	78.2	90.9
373	2.02	2.492	5.91	3.89	3.79	0.98	0.25	0.06	0.02	0.004	2.44	21.80	4.18	2.16	78.0	91.1
423	2.05	2.490	5.91	3.86	3.81	0.99	0.26	0.07	0.02	0.004	2.43	21.40	4.12	2.07	78.7	88.2
Rev*	1.99	2.504	5.87	3.88	3.79	0.98	0.25	0.06	0.02	0.004	2.46	21.80	4.14	2.15	78.2	90.3
523	1.97	2.522	5.82	3.85	3.81	0.99	0.26	0.07	0.02	0.004	2.48	21.20	3.95	1.98	79.7	83.7
Rev*	1.91	2.537	5.78	3.87	3.79	0.98	0.25	0.07	0.02	0.004	2.50	21.60	3.97	2.06	79.1	85.8

 $n_x$ —experimental value of  $n$ . $n_0$ —calculated value of  $n$ .

\*See Ref. (8) for details.

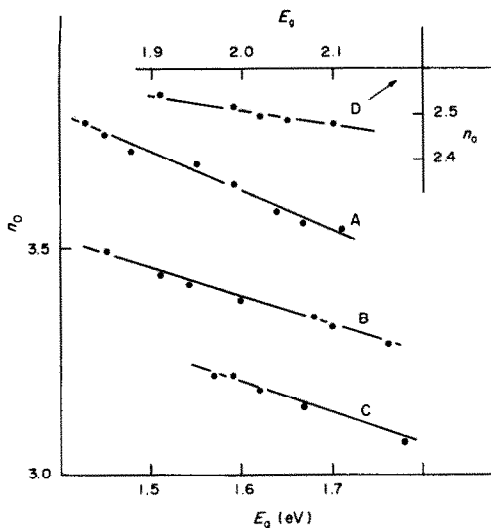


Fig. 3.  $E_g - n_0$  behaviour for different  $C/H$ , where  $n_0$  is the static refractive index (referred to as  $n$  in the text).

In Table 1, we present the results of our calculations of  $dn/dE_g$ . It is gratifying to note that the equation (21) is obeyed fairly well by samples containing hydrogen at 12 and 17 at.%. Of course, it should be pointed out here that the sample prepared at low  $T_s$  ( $50^\circ\text{C}$ ) is complex and may not be representative of a-Si:H. Such a linear dependence of  $n$  on  $E_g$  can also be seen to follow from relation (3) as also from the BBR (equation 5). For small changes in  $E_g$ , we have

$$n = A_1 + B_1 E_g \quad (22)$$

where  $A_1$  and  $B_1$  are constants.

As a concluding part of the present study, we now look at the application of the Wemple-Didomenico model to our samples. Based on their semi-empirical model, Wemple and Didomenico<sup>(4)</sup> proposed that

$$n^2(E) - 1 = \frac{E_d E_0}{E_0^2 - E^2} \quad (23)$$

where,  $E$  is the photon energy and the rest of the symbols have their usual meanings.<sup>(15)</sup> In Fig. 4, we plot  $1/[n^2(E) - 1]$  as a function of energy for various temperatures. As can be seen in the

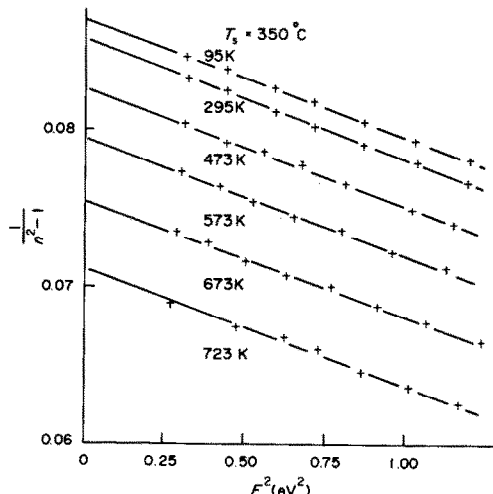


Fig. 4. Application of Wemple-Didomenico model to explain the variation of refractive index with (energy)<sup>2</sup> [ $C/H = 8\%$ ].

figure, the variation is linear and parallel. This reiterates our faith in the assumption that  $\hbar\omega_p \cong$  a constant. After all, equation (23) can be written as

$$\frac{1}{n^2(E) - 1} = \frac{E_0}{E_d} - \frac{E^2}{E_d E_0} \quad (24)$$

Thus the intercept and the slope yield  $E_0/E_d$  and  $1/E_d E_0$ , respectively. An evaluation of  $E_0$  and  $E_d$  is thus made possible. The reader may refer to the detailed work of Berger *et al.*<sup>(16)</sup> concerning these studies. Further, the fact that the lines are parallel implies that the product  $E_d E_0$  is a constant independent of measurement temperature. This is demonstrated in Table 1 for all samples prepared at various  $T_s$ . A comparison of the Penn model with the Wemple–Didomenico model yields a qualitative relation of the form

$$(\hbar\omega_p)^2 \cong E_d E_0 \quad (25)$$

The constancy of  $E_d E_0$  with temperature is hence explained. Note that with increase in measurement temperature, the refractive index and hence the dispersion energy  $E_d$  increases. Wemple–Didomenico define  $E_d$  as<sup>(15)</sup>

$$E_d = \beta' N_c N_v Z_a \quad (26)$$

where,  $\beta' = 0.37 \pm 0.04$  eV in covalent materials,  $N_c$  is the coordination number of the cation nearest neighbour to the anion,  $Z_a$  is the formal chemical valency of the anion and  $N_v$  is the total number of valence electrons per anion. Further,  $E_d$  is a parameter which has essentially been correlated with  $\epsilon_2$ . Thus, from the above definition, it follows that the temperature dependence of  $E_d$  may be because of the temperature dependence of  $N_c$ .

Using the arguments put forward by Wemple,<sup>(15)</sup> the increase in  $E_d$  (with  $T_m$ ) implies an increase in the coordination number (associated with complete or saturation of dangling bonds at void boundaries). In addition to  $N_c$ , we are of the opinion that the density will also have an impact on  $E_d$ . In Table 1, we present the mean values of some of the important parameters under consideration.

## CONCLUSION

In the above study, an analysis of the dependence of the index of refraction on the optical gap has been presented. This study has been carried out in the light of the models of Bahl–Bhagat, Penn, Wemple–Didomenico, Moss and Ravindra *et al.* Because of weaknesses associated with the fitting parameters in the Bahl–Bhagat model, an alternate model has been proposed. The Moss formula is shown to yield encouraging results. All these analyses have been carried out for the case of amorphous silicon produced by glow discharge with different hydrogen concentrations.

*Acknowledgements*—We are very thankful to Professor S. Robin for the fruitful discussions. We are grateful to Professor G. Weiser and Dr J. Beichler (Marburg, R.F.A.) for providing us the G.D. samples. One of the authors (NMR) gratefully acknowledges the financial support of C.I.E.S. (France).

## REFERENCES

1. S. K. Bahl and S. M. Bhagat, *J. Non-Crystall. Solids* **17**, 409 (1975).
2. P. M. Martin and W. T. Pawlewicz, *Solar Energy Mater.* **2**, 143 (1979/80).
3. D. R. Penn, *Phys. Rev.* **128**, 2093 (1962).
4. S. H. Wemple and M. Didomenico, *Phys. Rev.* **B3**, 1338 (1971).
5. N. M. Ravindra, *Infrared Phys.* **21**, 283 (1981) and references therein.
6. T. S. Moss, *Proc. Phys. Soc.* **B63**, 167 (1950).
7. A. Divrechy, B. Yous, J. M. Berger, J. P. Ferraton, J. Robin and A. Donnadieu, *Thin Solid Films* **78**, 235 (1981).
8. J. M. Berger, B. Yous, J. P. Ferraton and A. Donnadieu, *5th Int. Congr. on Physics of Non-Crystalline Solids*, Montpellier, July 1982 (to be published).
9. J. P. Ferraton, C. Ance and A. Donnadieu, *Thin Solid Films* **78**, 207 (1981).
10. T. S. Moss, *Optical Properties of Semiconductors*. Academic Press, New York (1959).
11. D. T. Pierce and W. E. Spicer, *Phys. Rev.* **B5**, 3017 (1972).
12. N. M. Ravindra, C. Ance, J. P. Ferraton, A. Donnadieu and S. Robin, *Phys. Status Solidi* **b115**, (1983).
13. C. Ance and N. M. Ravindra (communicated).
14. V. P. Gupta and N. M. Ravindra, *Phys. Status Solidi* **b100**, 715 (1980).
15. S. H. Wemple, *Phys. Rev.* **B7**, 3767 (1973).
16. J. M. Berger, J. P. Ferraton, B. Yous and A. Donnadieu, *Thin Solid Films* **86**, 337 (1981).